A99-31171

AIAA 99-2359

# Combustion and Flame Structure of HNF Sandwiches and Propellants

J. Louwers, G.M.H.J.L. Gadiot
TNO Prins Maurits Laboratory, Rijswijk, The Netherlands

A.J. Landman, T.W.J. Peeters, Th. H. van der Meer, D. Roekaerts
Delft University of Technology, Delft, The Netherlands

**35th AIAA/ASME/SAE/ASEE Joint Propulsion Conference and Exhibit**
**20–24 June 1999**
**Los Angeles, California**

AIAA 99-2359

# COMBUSTION AND FLAME STRUCTURE OF HNF SANDWICHES AND PROPELLANTS

J. Louwers*, G.M.H.J.L. Gadiot‡

*Research Group Rocket Technology, TNO Prins Maurits Laboratory*
*P.O. Box 45, 2280 AA Rijswijk, the Netherlands*

A.J. Landman¶, T.W.J. Peeters[1], Th. H. van der Meer#, D. Roekaerts**

*Thermal and Fluids Sciences, Department of Applied Physics, Delft University of Technology*
*P.O. Box 5046, 2600 GA Delft, the Netherlands*

## ABSTRACT

The combustion of hydrazinium nitroformate (HNF) sandwiches and HNF propellants has been studied in window bombs. Sandwich experiments were carried out up to 1 MPa. The binder in HNF/GAP sandwiches regresses along with the HNF. At the interface of GAP and HNF the regression rate is higher than that of neat HNF. Results of kinetic modeling of the HNF/GAP sandwich structure confirm that the final flame temperature is reached closer to the burning surface above the binder slab. The binder in HNF/HTPB sandwiches does not keep up with the oxidizer. The extension above the burning surface is dependent on the pressure. At increasing pressures, the protrusion decreases. HNF/GAP propellants with both coarse and fine (474μm and 100μm based on sphere volume) were made with a solid loading of 55%. Both propellants have a burn rate exponent n=0.68±0.02. The difference in burn rate is very small: the propellant with fine HNF burns 4% faster at 5 MPa. The burn rate exponent of a HNF/HTPB propellant containing 73% HTPB is n=1.01±0.05. The HTPB propellant has a lower regression rate than the GAP propellant. The sandwich and propellant results show that GAP actively participates in the combustion, whereas HTPB does not contribute to the combustion. NO*, OH* and CN* emission images show that only the GAP sandwich has a clear diffusion flame, close enough to the surface to affect burning rate. Emission images of propellants containing coarse HNF show that only part of the surface is burning simultaneously. The propellant containing fine HNF has a more homogeneous emission from the surface.

## INTRODUCTION

Most of today's rocket propellants are based on ammonium perchlorate (AP) with a non-energetic binder like hydroxy-terminated polybutadiene (HTPB). It is well known that the burn rate of AP/HTPB propellants is dependent on the AP particle size distribution [1]. The low flame temperature of the AP oxidizer flame and the high temperature of the final flame cause this strong dependence. In case of large AP particles, the cool AP flame is close to the surface, and the burning rate is low. In case of small AP particles a premixed mixture is formed, with a high flame temperature close to the burning surface. The heat feedback to the propellant surface is larger, and the regression rate becomes higher. This process is used to steer the burn rate of AP-based propellants (together with other methods, like adding catalysts).

For many propellants containing new energetic ingredients the effect of particle size is small, slightly positive or negative. Typical examples are HMX/HTPB propellants [2]. The burn rate sensitivity of these propellants to oxidizer particle size was found to be almost an order of magnitude smaller than that of AP/HTPB propellants.

* Ph.D. student, corresponding author, email: louwers@pml.tno.nl, phone: +31-15-2843367, fax: +31-15-2843958
‡ Senior propulsion engineer
¶ Student
[1] Assistant professor
# Associate professor
** Professor

In this paper the effect of oxidizer particle size on the combustion of Hydrazinium Nitroformate (HNF) based propellants is evaluated. HNF propellants have a higher performance than AP-based propellants [3-7]. Furthermore, the exhaust products are chlorine-free. Because of these advantages, HNF regained new interest. After introductory experiments at TNO/PML, a pilot plant was constructed at Aerosace Propulsion Products (APP) in the Netherlands [6,7]. Since then the HNF morphology and stability have been improved. This resulted in HNF/ Al (aluminum) / GAP (glycidyl azide polymer) propellants, containing 59% HNF, 23% GAP, and 18% Aluminum. It was shown that the performance of a HNF/GAP propellant is higher than that of a conventional AP/HTPB propellant [4]. The burn rate of these propellants was determined in small test motors, and a strand burner setup [8]. The burn rate exponent of this reference propellant was n=0.84. Replacing 4% aluminum with burn rate modifiers reduced the burn rate exponent to n=0.59.

To obtain a better understanding of the oxidizer-binder flame structure, sandwiches of oxidizer and fuel are often used. Sandwiches allow for a more accurate determination of the oxidizer-fuel interaction, as it is a two dimensional structure, as compared to the randomly distributed three dimensional structure normally present in propellants. The review of Price is a good summary of sandwich technology [9]. The two dimensional structure of sandwiches makes imaging possible. In a recent paper, the AP/Binder diffusion was studied by imaging the OH* emission [10]. This was shown to be a simple method to visualize the diffusion flame structure of AP-based sandwiches.

Parr and Hanson-Parr studied neat HNF and HNF sandwich flames by laser-induced fluorescence (LIF) and emission imaging [11,12]. The neat HNF flame was reported to be very short, with most chemical reactions occurring in a region up to a distance of 0.5 mm from the burning surface. The sandwich experiments showed that even non-energetic binders were consumed at 1 atm. At higher pressures, the non-energetic binders are left behind. For these binders the decomposition products escape through the diffusion flame. Energetic binders were found to keep up with the HNF surface, producing a stronger diffusion interaction.

Due to the supposed incompatibility of HNF with polybutadiene binders [13], energetic binders like GAP are usually used in HNF-propellants. However the TNO-Prins Maurits Laboratory (TNO/PML) recently found that it is possible to manufacture stable HNF/HTPB propellants. In this study, the flame structure of HNF propellants with both GAP and HTPB binder is determined.

This work focuses on the effect of varying HNF particle size on the combustion of HNF-based propellants. The flame temperature of the HNF oxidizer flame (2766 K at 0.1 MPa) is very close to that of the final diffusion flame for most propellants. Combined with the fact that the HNF flame structure is very short [10,11], it is expected that the effect of particle size in these propellants is much smaller.

In this study, experiments with HNF sandwiches have been carried out. Both sandwiches with an inert HTPB binder, as well as an energetic GAP binder have been tested. Combustion aspects of the sandwiches are studied by means of video images and emission images of excited OH*, CN* and NO*. The results of these experiments are compared to preliminary results of a computer model that is capable of calculating the gas phase above sandwich structures.

Experimental results for two different types of HNF-based propellants will be presented: a propellant based on an HTPB-binder, containing 73% HNF, and HNF propellants with a GAP-binder, containing 55% HNF. Also for the propellants video and emission images have been obtained. Furthermore, the burn rate of the propellants was determined in a strand burner. The experimental results are compared to results of a propellant model based on the BDP-model [1].

## EXPERIMENTAL

Regression rates were measured with a window strand burner at TNO/PML. This device is equipped with three polycarbonate (PC) windows of 150x15mm$^2$ and a thickness of 12mm. Maximum pressure in this strand burner is 20 MPa. Samples of approximately 10x10 mm$^2$ and a length of 100 mm were used. Ignition takes place by means of a nichrome wire. The regression rates are obtained from the recorded video images. The samples were inhibited with lead paint to prevent burning on the sides.

Flame structure visualization was carried out at Delft University of Technology (DUT). The DUT set-up uses a window bomb, which was especially designed for optical measurement techniques. Figure 1 shows a mechanical drawing of this bomb. The bomb is equipped with 4 sapphire windows of 50 mm diameter and 6 mm thickness, which are capable of withstanding pressures up to 5 MPa with a safety factor of 3. These windows are UV transparent down to approximately 220 nm. Before, during and after combustion the bomb is purged with nitrogen. Ignition and laser-assisted burning is accomplished by a $CO_2$-laser, which enters the bomb through a 10 mm thick zinc selenide (ZnSe) window on top of the bomb. The ZnSe window is flushed with nitrogen to prevent hot combustion gases reaching the window. Baffles are installed to prevent recirculation of the

combustion gases. Samples are placed on a post, which is inserted through the bottom of the bomb.

Figure 2 shows a schematic overview of the experimental setup. A Coherent Diamond G-50 $CO_2$ laser with an average output power of 50 W is used for ignition. The laser is controlled by an AED LC-C50 controller which allows modulation of the laser signal. A negative ZnSe lens diverges the laser beam to approximately 5 mm. The pressure in the bomb is measured with a pressure transducer (Omega PX213; range 1-1000 Psi). The combustion process is monitored by a color CCD camera (Hunt HTC-340). Video images are recorded on a digital video recorder (Sony DHR-1000). Burn rates are determined from the video recordings. Emission is collected and focused on the entrance slit of a high-resolution spectrometer (Jobin-Yvon THR-1000; 2400 gr/mm grating) equipped with an intensified diode array detector (Spectroscopy Instruments IRY 1024). The fluorescence can also be monitored on a low-resolution spectrometer (Jarrel Ash Monospec 18; 1200 gr/mm) also equipped with an intensified photodiode array detector (Princeton Instruments IPDA 1024). Both diode arrays use separate pulsers (Princeton Instruments FG-100) and share a common controller (Princeton Instruments ST-120). Emission images are obtained with an intensified CCD UV-sensitive camera (Princeton Instruments ICCD-576), and high speed 12 bits AD-converter (Princeton Instruments ST-138). Emission images are focussed on the intensifier plate by a 105mm/4.5 UV Nikon lens. To increase the magnification a bellows is used (Nikon PB6). The maximum resolution that can be obtained with this camera-lens-bellows combination is 10.75μm per pixel. The exposure time was 20-25 ms. Analog measurements (combustor pressure etc) are carried out using a 12-bit, 8 channel data acquisition board (National Instruments PCI-1200). The typical sampling rate is 1 kHz. All data acquisition and processing software is written in LabVIEW®.

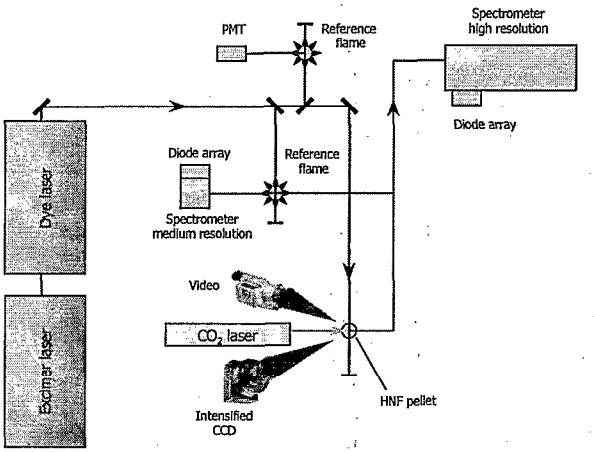


*Figure 2: Schematic overview of the experimental setup.*

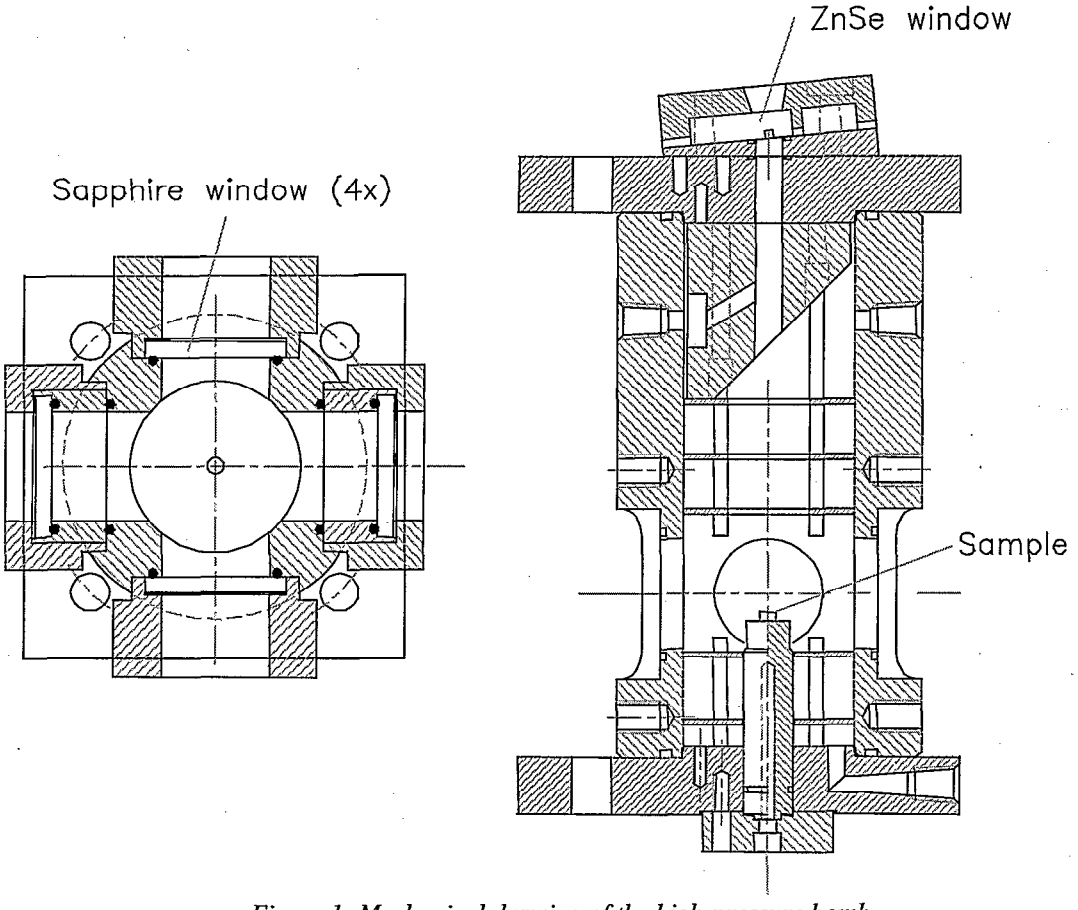


*Figure 1: Mechanical drawing of the high-pressure bomb.*

## SAMPLE PREPARATION

### SANDWICHES

Sandwiches were prepared by curing binder slabs between two oxidizer pellets. First, cylindrical HNF samples were pressed with a diameter of 6 mm and 3 mm thickness under high pressure (190 MPa). This results in pellets with 97% of TMD. Two of these pellets are then glued together with an uncured mixture of binder ingredients. The sandwich thickness is controlled by spacers between the two halves.

Initial experiments with a mixture of GAP and an isocyanate showed migration of binder ingredients into the oxidizer pellets. This migration is caused by the capillaries of the oxidizer samples. The result was breakdown of the pressed HNF pellets. In the end only a small amount of red liquid material remained. Most probably the isocyanate migrated out of the binder mixture into the oxidizer. The incompatibility of HNF with isocyanates explains the degradation reaction[6]. The problem of migration was solved by adding more curing catalyst to the binder mixture. Sandwiches of good quality could be obtained when using a binder mixture with a pot life of less than 20 minutes at room temperature. After curing, two flat sides are sanded to the sandwich at the position of the spacer. The sandwich is then mounted upright on one of the flat sides. The other flat side (top) is ignited by the $CO_2$-laser. Figure 3 shows an assembled HNF/GAP sandwich (binder about 1 mm thick).

Two sandwich combinations were selected: one containing a non-energetic binder (HTPB), and the other containing an energetic binder (GAP). All sandwiches were made with a binder slab thickness of 250 μm.

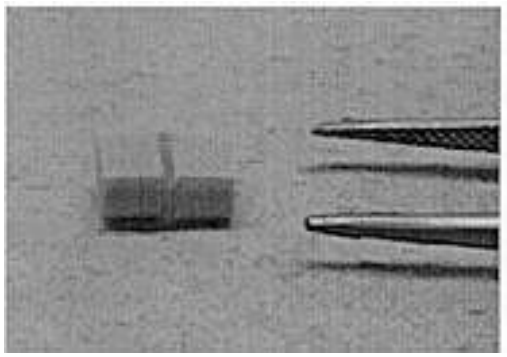

*Figure 3: Assembled HNF/GAP sandwich.*

### HNF PROPELLANTS

Two types of HNF propellants were used in this work. First, an HTPB-based propellant with a solid loading of 75%. This propellant contains a bimodal mixture of coarse HNF (474μm, type C15) and fine HNF (100μm, type S16). The HNF particles are needle shaped. These two grades have an L/D of 5. The particle size is based on an equivalent spherical volume. The propellant formulation is summarized in Table 1.

*Table 1: Formulation of HTPB-based propellant.*

| *Material* | *composition [%]* | *composition [%]* |
|---|---|---|
| *Bimodal HNF* | 73 | |
| *HNF C15 + S16* | | |
| *Additives* | 2 | |
| *Binder* | 25 | |
| *HTPB + isocyanate* | | 80 |
| *Plasticizer* | | 20 |

The other propellant formulation contains the energetic binder GAP. To determine whether the HNF particle size affects the burn rate, two propellants were manufactured with the above mentioned different HNF types available. To allow for a good comparison, the solid loading for both propellants was the same. Because of the monomodal particle size distribution and the viscous GAP binder, the maximum solid loading that could be obtained was 55%. Table 2 summarizes the HNF/GAP composition.

*Table 2: Formulation of GAP-based propellants.*

| *Material* | *prop. 1 composition [%]* | *prop. 2 composition [%]* |
|---|---|---|
| *HNF* | | |
| *HNF C15* | 55 | |
| *HNF S16* | | 55 |
| *Binder* | | |
| *GAP + isocyanate* | 45 | 45 |

The propellants were prepared in a small mixer in 300 gram batch size. Mixing took place under vacuum conditions. After mixing the propellants are poured in a casting mold and cured to a single piece of propellant with dimensions of approximately 30x40x150 $mm^2$. The propellant is then cut into strand burner samples, and slices of 4 mm thickness. From these slices cylindrical samples with a diameter of 6 mm are made which are used for the flame visualization experiments.

# RESULTS

## HNF SANDWICHES

HNF/GAP sandwiches with a 250 μm binder lamina were burned at different pressures. The video images of these experiments are shown in Fig. 4. (Note that all images were obtained using different lens aperture settings due to the increasing flame luminosity with increasing pressure.) The experiments show that the GAP binder regresses along with the HNF surface. At the binder/oxidizer interface, the HNF regresses faster than at some distance from the binder. However a diffusion flame is not visible in the wavelength range of visible light.

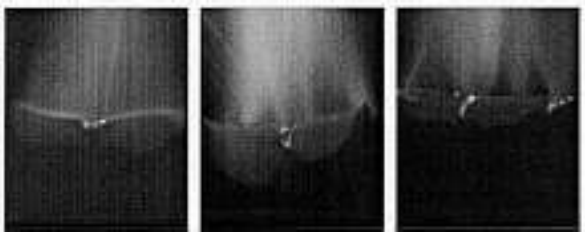

*Figure 4: Video images from sandwiches of HNF and GAP at 0.12, 0.3, and 1.0 MPa. (image size = 8.4 x 6.9 mm$^2$)*

To further resolve a possible diffusion interaction in these sandwiches, emission images were obtained for different radicals. An interference filter centered at 241.5 nm, and a FWHM of 18 nm was used to visualize the chemiluminescence of the γ-bands of NO. The chemiluminescence of the A←X transition of OH was determined by an interference filter centered at 310 nm, and a FWHM of 20 nm. Emission from CN was detected through a combination of Shott filters UG-11 and GG-375. This combination forms a band pass filter, centered at 385 nm, and a FWHM of approximately 20 nm. This passes the chemiluminescence of the B←X transition of excited CN at 388 nm.

Figure 5 shows the CN, OH, and NO emission images of HNF / GAP sandwiches at 0.12 MPa. All three radicals show an intense bright emission above the burning surface of HNF. CN and OH also have a continuous emission above the burning surface. Only the NO emission reveals the diffusion interaction pattern. The sequences shown in Figure 6 and 7 allow further comparison of the OH emission images and NO emission images. These sequences also show that the NO emission yields more information about the flame structure of the diffusion flame.

As mentioned, the HNF/GAP sandwiches show a higher regression rate near the binder-fuel surface. This results in an increasing V-shape during combustion (see e.g. Fig. 6 and 7). It has been reported that the regression rate of HNF with additives is higher than that of neat HNF [14]. The cause of this is a higher heat feedback to the burning surface, due to a steeper temperature profile in the presence of a fuel. A similar mechanism probably causes the HNF/GAP interface regression rate to be higher as well.

Because NO emission shows the diffusion pattern most clearly, it was decided only to measure NO emission images for the HNF/HTPB sandwiches.

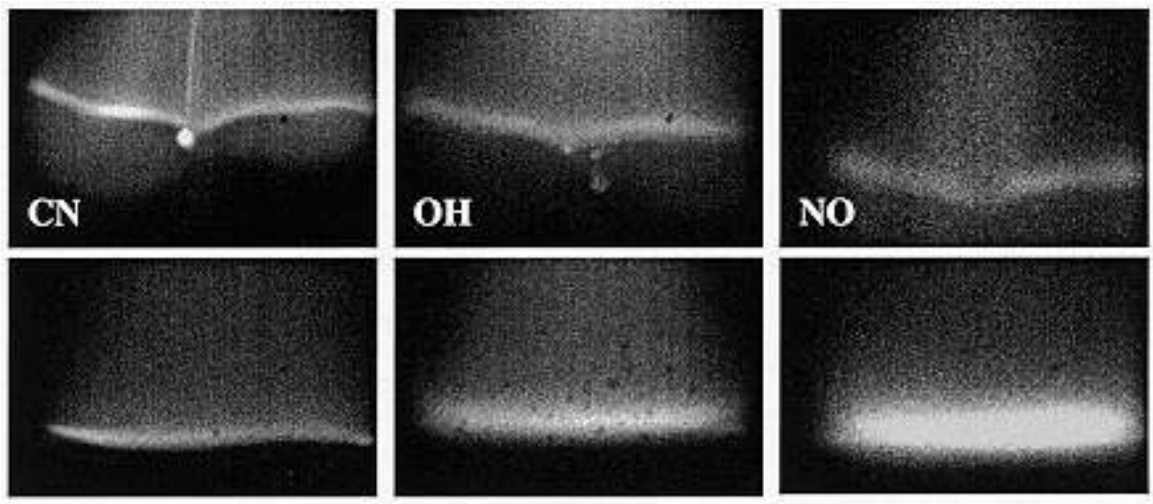


*Figure 5: Emission of HNF/GAP sandwich at 0.12 MPa. From left to right: CN, OH and NO emission. As a reference, the emission images of neat HNF are also given at the lower row. Image size is 4.1 x 6.2 mm$^2$.*

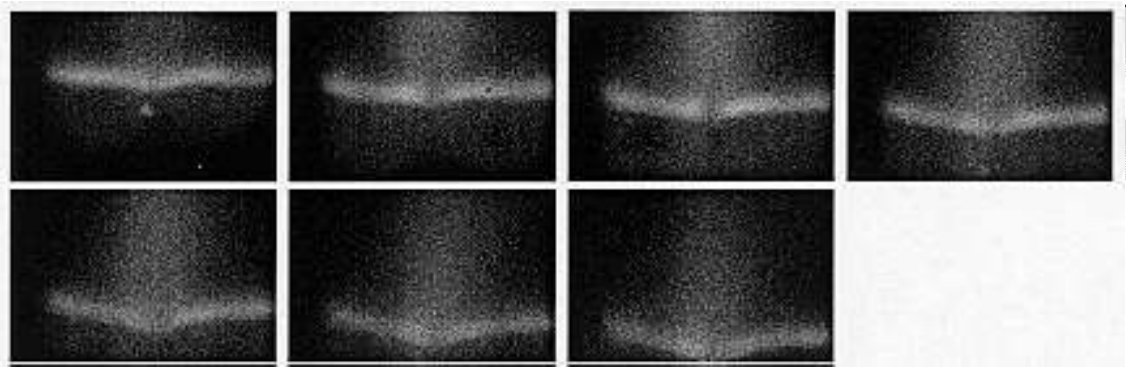

*Figure 6: Sequence of NO emission of HNF/GAP sandwich at 0.12 MPa. Image size is 4.1 x 6.2 mm$^2$.*

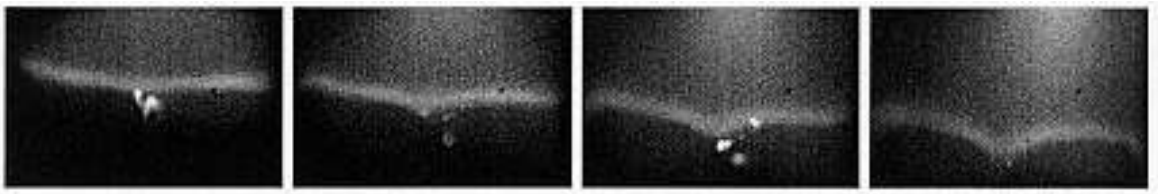

*Figure 7: Sequence of OH emission of HNF/GAP sandwich at 0.12 MPa. Image size is 4.1 x 6.2 mm$^2$.*

Video images of HNF/HTPB sandwiches are shown in Fig. 8. These images show that the HTPB binder slab extends above the burning surface of HNF. Above the HTPB binder a very bright diffusion flame is visible. The flame standoff (from binder surface to luminous flame) and binder protrusion decrease with increasing pressure, see Fig. 9.

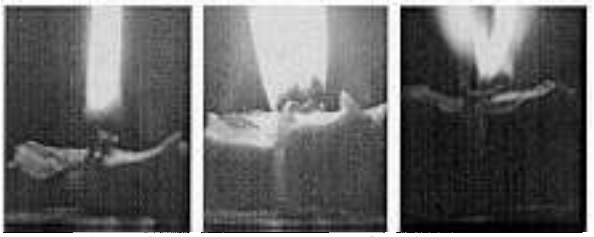

*Figure 8: Video images from sandwiches of HNF and HTPB at 0.12, 0.3, and 1.0 MPa. (image size = 8.4 x 6.9 mm$^2$)*

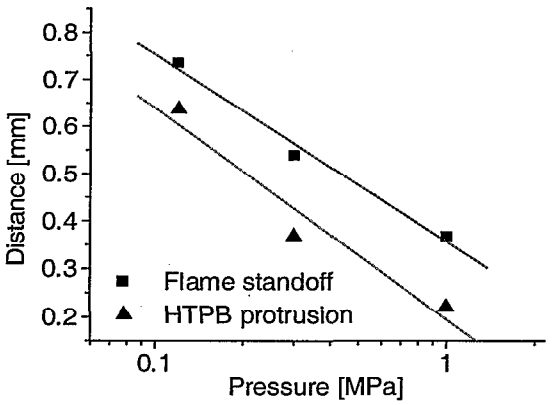


*Figure 9: Flame standoff and binder protrusion of a HNF / HTPB sandwich.*

The NO emission images showed a very bright diffusion flame, Fig. 10. The emission from the luminous flame makes it difficult to detect the emission from NO in the neat HNF flame. The diffusion flame with the HTPB binder is further away from the burning surface, and less pronounced that that with a GAP binder. These observations are in agreement with the results from Parr and Hanson-Parr [8].

*Figure 10: NO emission images from sandwiches of HNF and HTPB at 0.12, 0.3, and 1.0 MPa. (image height 4.1 mm).*

It was attempted to make sandwiches from loosely stacked binder and fuel slabs. If the contact between binder and oxidizer was not very good, combustion usually also occurs at the interface between binder and oxidizer. A few sandwiches were made with the binder slab glued to the oxidizer pellets with a small amount of cyanoacrylate glue. Even the smallest amount that could be applied left a carbonaceous material. The flame also becomes much brighter, as shown in Fig. 11. This flame nicely shows the diffusion pattern.

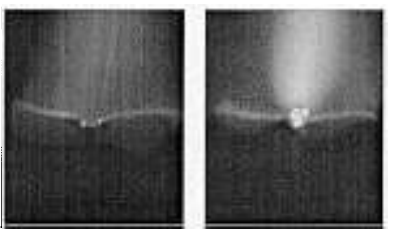

*Figure 11: Left: HNF/GAP sandwich at 0.12 MPa. Right: HNF/GAP sandwich with sandwich glued to the pressed oxidizer pellets. (image size = 8.4 x 6.9 mm$^2$)*

The BIGMIX code of Delft University of Technology has been developed for the calculation of turbulent diffusion flames [15]. The program was modified to be able to use it for the laminar HNF/GAP diffusion flame in a sandwich. A chemical database was constructed, based on Yetter's kinetics for nitramines, and the GRI-mech for hydrocarbon combustion [16,17].

The BIGMIX code is only capable of calculating the gas phase. As boundary conditions, the surface temperatures of HNF and GAP were used. Earlier calculations had shown that HNF only partially decomposes in the condensed phase, and that most of the decomposition takes place in the gas phase [18]. The boundary conditions for GAP were determined from measurements as summarized in the paper of Davidson and Beckstead [19]. The experimental results of Kubota and Sonobe were used as input for the surface temperature of GAP [20].

The temperature distribution in Fig. 12 shows that the final flame temperature is reached closer to the burning surface above the binder slab (see iso-temperature line). This corresponds to the higher regression rates of the HNF/GAP sandwich close to the binder. The mean mixture fraction profile resembles the flame seen in Fig. 11. The CN profile is a good indication of the position of the diffusion flame. Note that this profile is very different from the CN* emission profile. In the future CN-LIF measurements will be carried out to measure the CN profile (Fig. 5).

The computational grid is shown in the last image of Fig. 12, together with the HNF mass fraction. HNF decomposes rapidly above the burning surface, but is not responsible for the higher temperatures around the interface, as the HNF decomposition is slower around this interface.

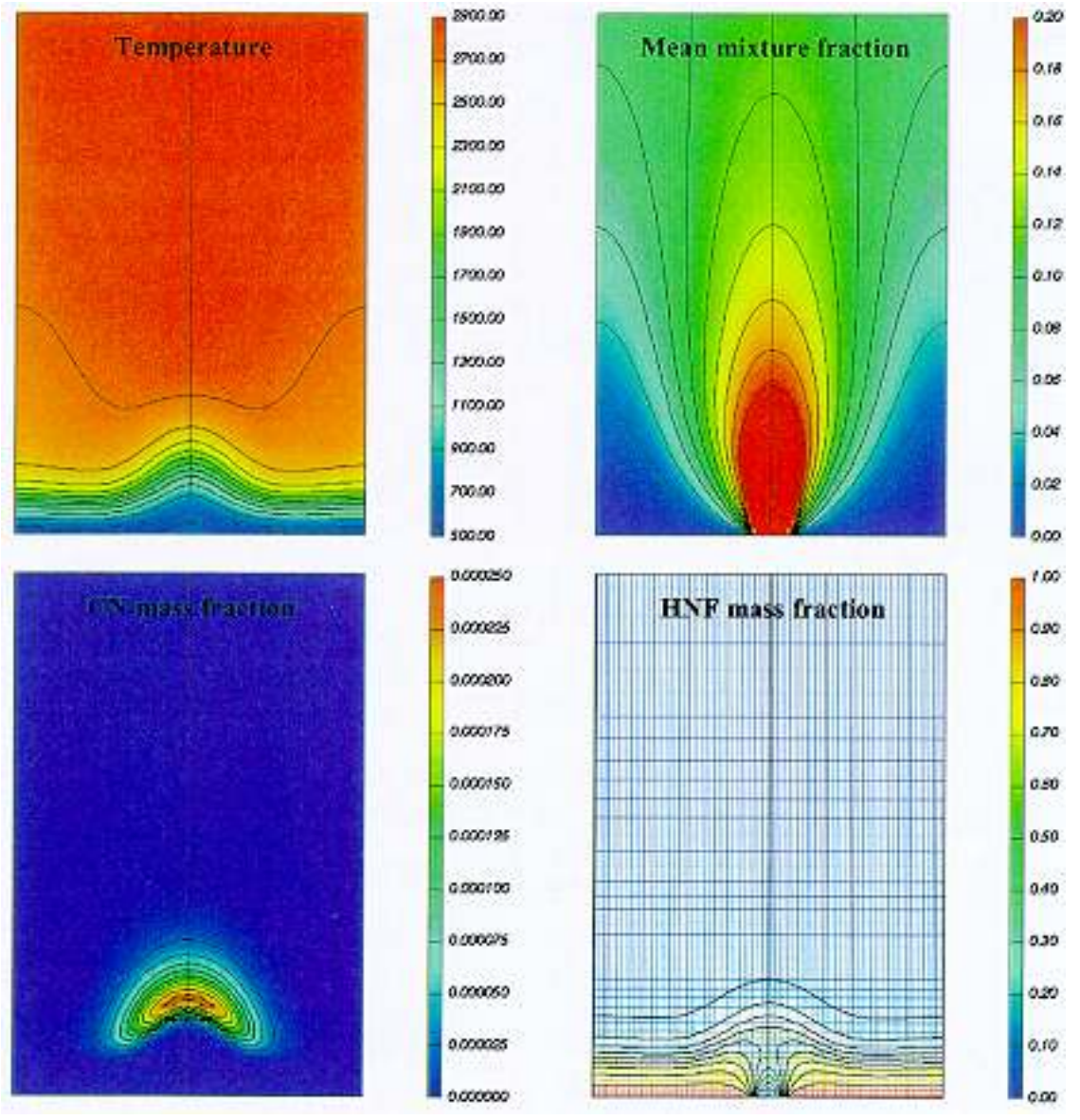


*Figure 12: From left to right: Bigmix calculations of HNF/GAP sandwich at 0.1 MPa. Image size represents 2 x 3 mm$^2$. The GAP binder slab is 200μm thick. Shown are temperature, mean mixture fraction, CN mass fraction, and HNF mass fraction (with computational grid).*

## HNF PROPELLANTS

Figure 13 shows video images of the HNF/GAP propellants for the two different types of HNF (C15 coarse, S16 fine) in comparison with images of neat HNF. The propellant with fine HNF did not burn self-sustained when the $CO_2$-laser was switched of below 0.3 MPa. The image at 0.12 MPa for this propellant was obtained with the $CO_2$-laser operating.

The flame of neat HNF is brighter than that of the HNF/GAP propellants. The neat HNF has a bluish color at all pressures. This emission comes from CN* and CH* radicals [10,14]. This bluish color only becomes visible at elevated pressures in the HNF propellants. The propellant with the coarse HNF shows a heterogeneous flame structure. Except for the CN* emission, the emission from neat HNF is stronger than that of the propellants. This is caused by the continuous emission from the protruding binder. The UG-11 filter used for the CN emission also passes some light around 600 nm.

When emission images are compared, it becomes clear that in case of the coarse HNF not the whole surface of the propellant is burning. Only at localized spots there is emission from the surface. A typical example of this is shown in Fig. 14. The size of the emission spots matches the HNF particle size. Another example is shown in Fig. 15. This shows the OH emission image of a HNF propellant burning at an angle. The needle-shaped particles can be recognized at some points in this figure.

The propellant with the fine HNF shows a much more homogenous emission from the burning surface. This difference can be explained by the fact that the regression rate of HNF is very high. Once ignited, a particle burns very fast. Regression rate is more determined by the ignition delay of the particle, rather than the intrinsic burn rate. Similar results were also found for propellants containing nitramines [2]. Neat HNF has an even higher regression rate than the nitramines.

The regression rate of both HNF/GAP propellants is shown in Fig. 16. For the propellant with coarse HNF C15 the burning rate exponent is n=0.69±0.02. The propellant containing fine HNF has the same burn rate exponent n=0.68±0.01. For reference the regression rate of neat HNF and GAP are also shown [20-22]. The difference in regression rate between the coarse and fine HNF is very small. At 5 MPa the absolute difference is 0.7 mm/s, with an average regression rate of 17.5 mm/s.

At low pressures, the addition of fuel to HNF causes a steeper temperature gradient, causing the burn rate to be higher than that of neat HNF. As the pressure increases, NO reactions become faster, and the effect of additional fuel reduces [14]. The sandwich experiments also show that around the HNF/GAP surface the burn rate is higher. So, at low pressures the burn rate is enhanced by the presence of GAP, whereas at high pressures, the binder slows down the combustion.

*Figure 15: OH emission of HNF C15 / GAP propellant at 0.15 MPa (image size = 4.1 x 6.2 mm$^2$).*

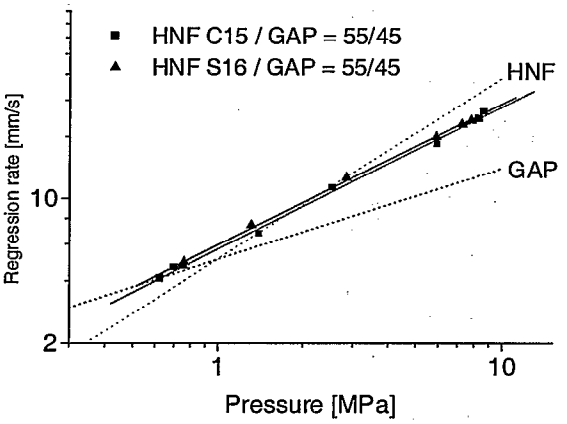


*Figure 16: Regression rate of HNF / GAP propellants compared to that of neat HNF and GAP.*

*Figure 14: OH emission at 0.3 MPa. From left to right: HNF, HNF C15 / GAP and HNF S16 / GAP. (image size 4.1 x 6.2 mm$^2$)*

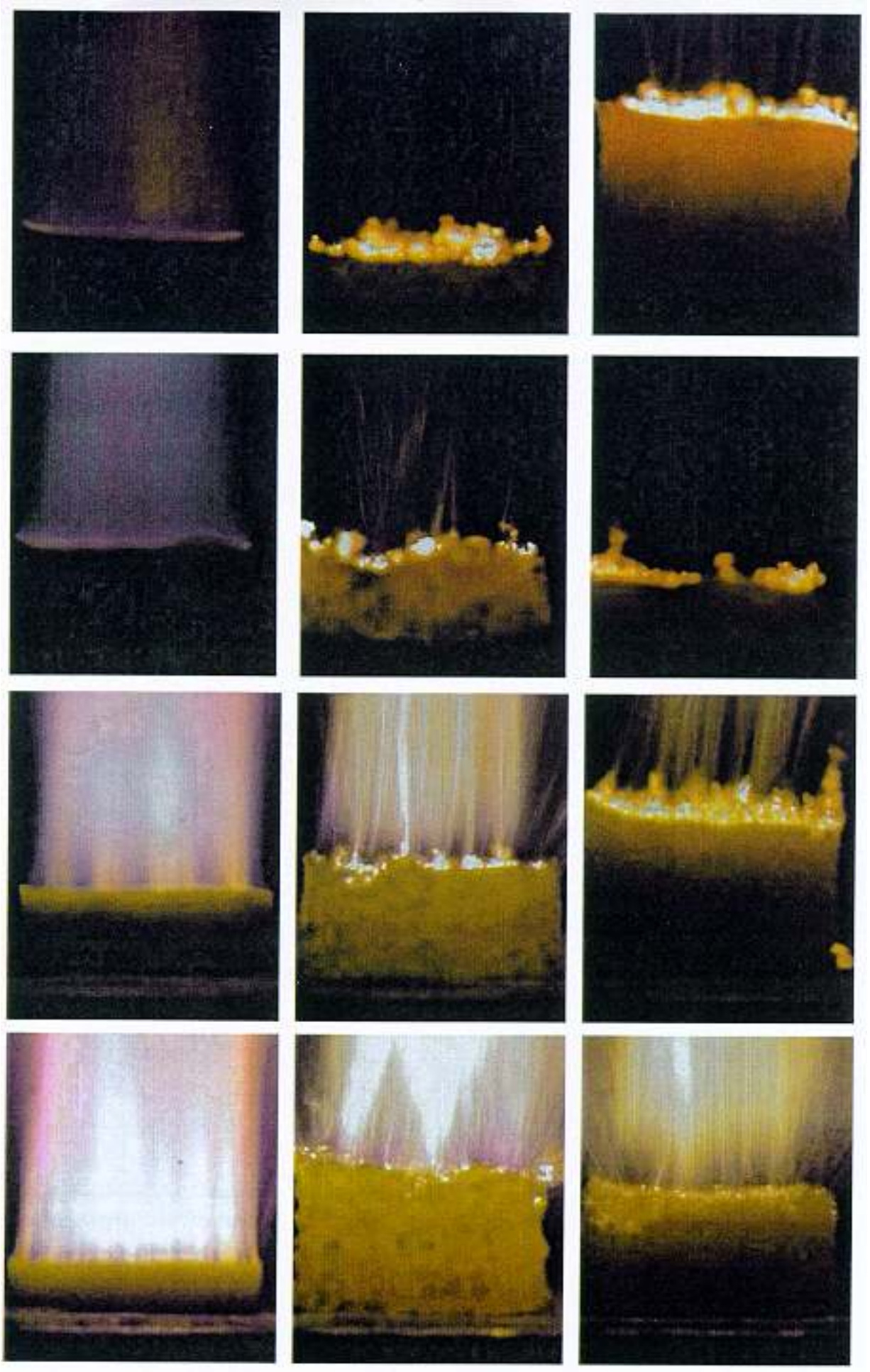

*Figure 13: From left to right: Video images of HNF, HNF C15 / GAP, and HNF S16 / GAP. From top to bottom: 0.12 MPa, 0.3 MPa, 0.9 MPa, and 2.0 MPa. The image at 0.12 MPa with S16 was obtained with $CO_2$ –laser switched on. (image size 8.4 x 6.9 $mm^2$)*

Figure 17 shows the results of a BDP-type of model [1]. In this model it has been assumed that only two of the classical three flames are present: oxidizer flame, and final diffusion flame. The primary diffusion flame between a small amount of oxidizer and binder products has been neglected ($\beta_f$=0). As found experimentally the difference in burning rate is small.

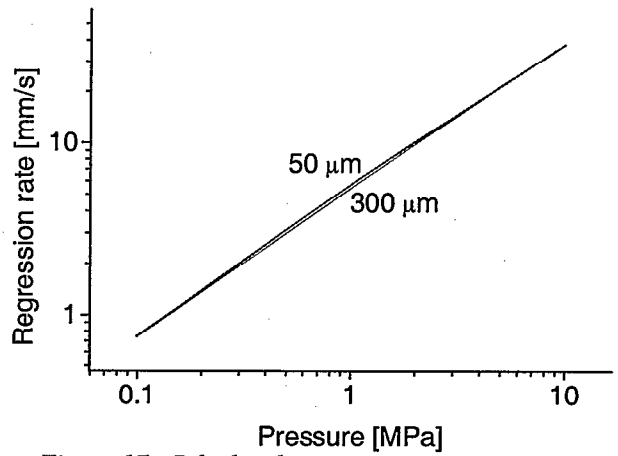


*Figure 17: Calculated regression rate of HNF/GAP =55/45 propellant with different particle size.*

The contribution of the two flames at 1 MPa is shown in Fig. 18. When the oxidizer particles are larger than 200µm the burn rate is determined solely by the HNF flame. With increasing pressure, the point above which the diffusion flame becomes unimportant shifts to smaller particle sizes.

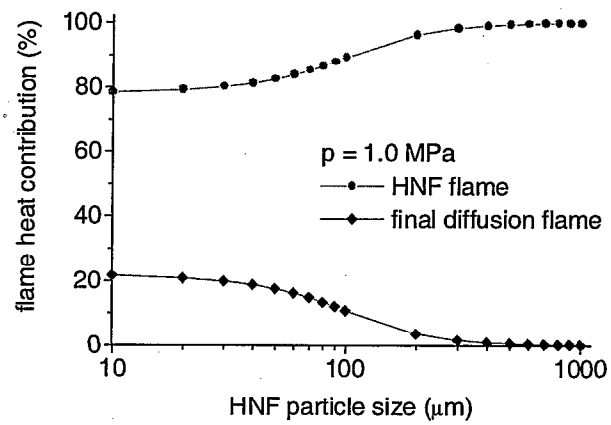


*Figure 18: Modeled contribution to the heat feedback of the two flames of a HNF / GAP propellant.*

The measured burn rate of the HTPB propellant is shown in Fig. 19. Compared to the GAP-based propellant the burn rate is much lower, although the HNF oxidizer content is 73% compared to 55% in the GAP propellant. This is in agreement with the sandwich results which showed a protruding HTPB binder that does not take part in the combustion process close to the burning surface. The burn rate exponent of this propellant is also higher n=1.01±0.05. This pressure exponent resembles that of neat HNF (0.85-0.90). This again indicates that the HTPB does not contribute as an active ingredient.

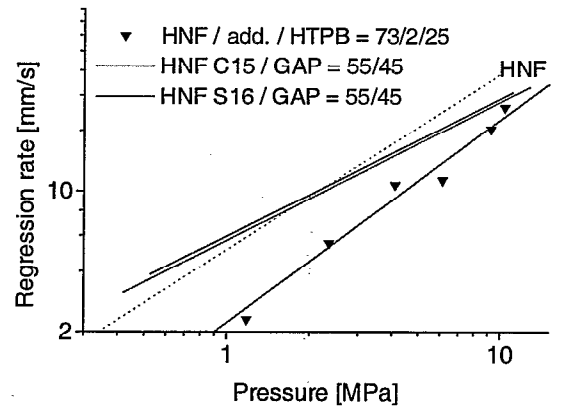


*Figure 19: Regression rate of HNF / HTPB propellants compared to that of neat HNF and GAP – based propellants.*

The propellant containing HTPB left a residue behind after combustion. Due to this residue it was impossible to determine the structure of the flame zone from video or emission imaging. Figure 20 shows the remaining mass residue as a function of combustion pressure. Below 0.5 MPa the combustion is smoldering, producing a yellow sooth in the combustor. Most probably this is HNF vapor, which has also been observed during neat HNF combustion [18]. Above 0.5 MPa flames become visible. The residue above 1 MPa is probably caused by 1% of non-combustible additive that is present in this propellant. When this propellant was burned in air, luminous flames were also observed below 0.5 MPa.

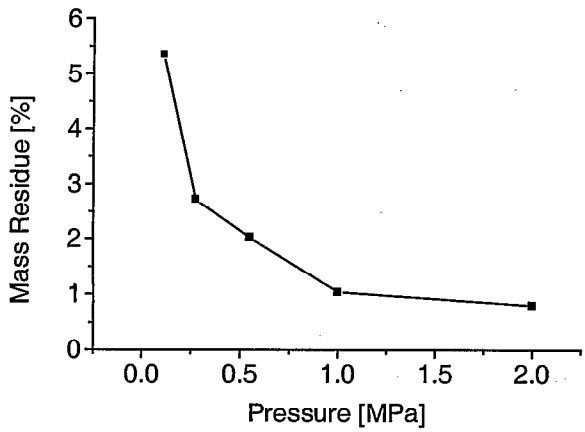


*Figure 20: Mass residue of HNF/HTPB propellant.*

## CONCLUSIONS

The combustion of hydrazinium nitroformate (HNF) sandwiches and HNF propellants has been studied in window bombs. Sandwich experiments were carried out up to 1 MPa. The binder in HNF/GAP sandwiches regresses along with the HNF. At the interface of GAP and HNF the regression rate is higher than that of neat HNF. Results of kinetic modeling of the HNF/GAP sandwich structure confirm that the final flame temperature is reached closer to the burning surface above the binder slab. The binder in HNF/HTPB sandwiches does not burn along with the oxidizer. The extension above the burning surface is dependent on the pressure. At increasing pressures, the protrusion decreases.

HNF/GAP propellants with both coarse and fine (474μm and 100μm based on sphere volume) were made with a solid loading of 55%. Both propellants have a burn rate exponent n=0.68±0.02. The difference in burn rate is very small: the propellant with fine HNF burns 4% faster at 5 MPa. The burn rate exponent of a HNF/HTPB propellant containing 73% HTPB is n=1.01±0.05. The HTPB propellant has a lower regression rate than the GAP propellant. The sandwich and propellant results show that GAP actively participates in the combustion, whereas HTPB does not contribute to the combustion.

NO*, OH* and CN* emission images show that only the GAP sandwich has a clear diffusion flame, close enough to the surface to affect burning rate. Emission images of propellants containing coarse HNF show that only part of the surface is burning simultaneously. The propellant containing fine HNF has a more homogeneous emission from the surface.

## ACKNOWLEDGMENTS

This work was sponsored by the Dutch Technology Foundation, STW under project DTN 66.4108. We would like to thank Aerospace Propulsion Products (APP) for providing the HNF for this work; The pyrotechnics and energetic materials group (TNO/PML-PE) for use of their fascilities; in particular Arnold Leeuwenburgh for preparation of the HNF propellants; Jaap Varkevisser for carrying out the strand burner experiments.

## REFERENCES

[1] M.W. Beckstead, R.L. Derr, and C.F. Price, *A Model of Composite Solid-Propellant Combustion Based on Multiple Flames,* AIAA Journal **9**, 2200, 1974.

[2] F.S Blomshield, *Nitramine Composite Solid Propellant Modelling,* NWC Report TP 6992, 1989.

[3] J.M. Mul, P.A.O.G. Korting, and H.F.R. Schöyer, *Search for New Storable High Performance Propellants,* AIAA Paper 88-3354, Boston, Massachusetts, 1988.

[4] H.F.R. Schöyer, A.J. Schnorhk, P.A.O.G. Korting, P.J. van Lit, *First Experimental Results of an HNF/Al/GAP Solid Rocket Propellant,* AIAA Paper 97-3131, Seattle, Washington, 1997.

[5] G.M.H.J.L. Gadiot, J.M. Mul, J.J. Meulenbrugge, P.A.O.G. Korting, A.J. Schnorhk and H.F.R. Schöyer, *New Solid Propellants Based on Energetic Binders and HNF,* IAF Paper IAF 92-0633, 1992.

[6] H.F.R. Schöyer, A.J. Schnorhk, P.A.O.G. Korting, P.J. van Lit, J.M. Mul, G.M.H.J.L. Gadiot and J.J. Meulenbrugge, *Development of Hydrazinium Nitroformate Based Solid Propellants,* AIAA Paper 95-2864, San Diego, California, 1995.

[7] H.F.R. Schöyer, A.J. Schnorhk, P.A.O.G. Korting, P.J. van Lit, J.M. Mul, G.M.H.J.L. Gadiot and J.J. Meulenbrugge, *High-Performance Propellants Based on Hydrazinium Nitroformate,* J. Prop. Power **11**, 856-859, 1995.

[8] G.M.H.J.L. Gadiot and L.J. Keus, *HNF/Al/GAP Propellant Pressure Sensitivity and Proof of Concept Work,* APP Report NP HG TER 00 02 021 (3), Hoogerheide, The Netherlands, 1996.

[9] E.W. Price, *Review of sandwich burning,* 30th Jannaf Combustion Subcommittee Meeting, Volume II, pp. 259-279, Naval Postgraduate School, Monterey, CA, 15-19 November, 1993.

[10] B.T. Chorpening, and M.Q. Brewster, *Flame Structure of AP/Binder Sandwiches from Emission Imaging,* AIAA Paper 99-0594, 1999.

[11] T.P. Parr and D.M. Hanson-Parr, *HNF: Neat and Diffusion Flame Structure,* 32nd JANNAF Combustion Subcommittee Meeting, 1995.

[12] T.P. Parr and D.M. Hanson-Parr, *Solid Propellant Diffusion Flame Structure,* 26th Int. Symp. on Combustion, July 28 – August 2, Naples, Italy.

[13] G.M. Low, *Hydrazinium Nitroformate Propellant with Saturated Polymeric Hydrocarbon Binder,* U.S. Patent 3,708,359, Jan 2, 1973.

[14] J. Louwers, G.M.H.J.L. Gadiot, M. Versluis, A.J. Landman, Th. H. van der Meer, D. Roekaerts, *Combustion of Hydrazinium Nitroformate Based Compositions,* AIAA 98-3385, 1998.

[15] T. Peeters, *Numerical Modeling of Turbulent Natural-gas Diffusion Flames,* Ph.D. Thesis, Delft University of Technology, Delft, The Netherlands, 1995.

[16] R.A. Yetter, F.L. Dryer, M.T. Allen, and J.L. Gato, *Development of Gas-Phase Reaction Mechanisms for Nitramine Combustion,* J. Prop. Power **11**, 683-697, 1995.

[17] C.T. Bowman, R.K. Hanson, D.F. Davidson, W.C. Gardiner Jr., V. Lissianski, G.P. Smith, D.M. Golden, M. Frenklach and M. Goldenberg, http://www.me.berkely.edu/gri_mech/ .

[18] J. Louwers, T. Parr, and D. Hanson-Parr, Decomposition and Flame Structure of Hydrazinium Nitroformate, AIAA Paper 99-1091, 1999.
[19] J. Davidson and M. Beckstead, *A Mechanism for GAP Combustion,* AIAA Paper 97-0592, 1997.
[20] N. Kubota and T. Sonobe, *Combustion Mechanism of Azide Polymer,* Prop. Exp. Pyr. **13**, pp 172-177, 1988.
[21] J.C. Finlinson and A.I. Atwood, *HNF Burnrate, Temperature Sensitivity, and Laser Recoil Response from 1 to 6 atm,* 34th JANNAF Comb. Meeting, West Palm Beach, Florida, 27-31 Oct. 1997.
[22] J. Louwers, G.M.H.J.L. Gadiot M.Q. Brewster, S.F. Son, *Model for Steady-State HNF Combustion,* Int. Workshop on Combustion Instability of Solid Propellants and Rocket Motors, Politecnico di Milano, Italy, 16-19 June 1997.

## ACRONYMS

| | |
|---|---|
| AP | Ammonium Perchlorate |
| APP | Aerospace Propulsion Products |
| DUT | Delft University of Technology |
| FWHM | Full width at half maximum |
| GAP | Glycidyl Azide Polymer |
| HMX | Cyclotetramethylene Tetranitramine |
| HNF | Hydrazinium Nitroformate |
| HTPB | Hydroxy-Terminated Polybutadiene |
| LIF | Laser-Induced Fluorescence |
| PML | Prins Maurits Laboratory |
| TMD | Theoretical Maximum Density |
| ZnSe | Zinc Selenide |